

Electronic Supplement 6

The dual-band method: Worked examples

In Chapter 4 we set up a “dual-band solution” for a mixed pixel containing two distinct thermal components using the following simultaneous Equations:

$$M(\lambda_1, T_{\text{int}}) = pM(\lambda_1, T_h) + (1 - p)M(\lambda_1, T_c) \quad (\text{S6.1a})$$

$$M(\lambda_2, T_{\text{int}}) = pM(\lambda_2, T_h) + (1 - p)M(\lambda_2, T_c) \quad (\text{S6.1b})$$

The solution we worked through in Chapter 4 involved assuming T_c to solve for the unknowns p and T_h . I give the IDL code that achieves this solution in Table S6.1. In this supplement we work through two other variants on this solution, where (1) T_h is assumed to solve for p and T_c , and then (2) p is assumed to solve for T_c and T_h .

I end this supplement by considering a few worked examples of thermal mixture modeling that use satellite sensor data for hot volcanic targets. These reveal the reality of the situation, and the limits within which we must operate, as forced by non-detection and saturation issues.

Dual-Band solution by assuming T_h or p

If T_h or p can be assumed we can re-arrange Equations (S6.1a) and (S6.1b) to isolate T_c , so that:

$$M(\lambda_1, T_c) = \frac{M(\lambda_1, T_{\text{int}}) - pM(\lambda_1, T_h)}{(1 - p)} \quad (\text{S6.2a})$$

$$M(\lambda_2, T_c) = \frac{M(\lambda_2, T_{\text{int}}) - pM(\lambda_2, T_h)}{(1 - p)} \quad (\text{S6.2b})$$

For solution we now have one of two options:

1. If T_h is known, T_h can be assumed and we can solve for T_c by iterating on p , or
2. If p is known, p can be assumed and we can solve for T_c by iterating on T_h .

Table S6.1. Sample code to solve the dual-band method by assuming T_c and iterating on T_h (written in IDL).

Code	Comment
Initialization	
cw1 = 3.75E-06	Input mid-point of band 1 waveband (in meters)
cw2 = 1.10E-05	Input mid-point of band 2 waveband (in meters)
BT1 = 248.0 + 273.15	Input band 1 pixel-integrated temperature (BT1 in Kelvin)
BT2 = 58.0 + 273.15	Input band 2 pixel-integrated temperature (BT2 in Kelvin)
Tc = 25.0 + 273.15	Input cold component temperature (Tc in Kelvin)
Thstart = Tc + 1.0	Set hot component temperature to 1 K greater than Tc (Th in Kelvin)
IF (Thstart LT BT1) THEN Thstart= BT1 ELSE Thstart = Thstart	Check that Th is greater than BT1, if not then set Th to BT1 + 1 K
IF (Thstart LT BT2) THEN Thstart= BT2 ELSE Thstart = Thstart	Check that Th is greater than BT2, if not then set Th to BT2 + 1 K
R1 = 0.00000000000000003741*cw1^(-5./ (EXP(0.014393/(cw1*BT1))-1.)	Convert BT1 to band 1 spectral radiant exitance (R1 in $W m^{-2} m^{-1}$)
R2 = 0.00000000000000003741*cw2^(-5./ (EXP(0.014393/(cw2*BT2))-1.)	Convert BT1 to band 2 spectral radiant exitance (R2 in $W m^{-2} m^{-1}$)
Rc1 = 0.00000000000000003741*cw1^(-5./ (EXP(0.014393/(cw1*Tc))-1.)	Convert Tc to band 1 spectral radiant exitance (Rc1 in $W m^{-2} m^{-1}$)
Rc2 = 0.00000000000000003741*cw2^(-5./ (EXP(0.014393/(cw2*Tc))-1.)	Convert Tc to band 2 spectral radiant exitance (Rc2 in $W m^{-2} m^{-1}$)
Rhstart1 = 0.00000000000000003741*cw1^(-5./ (EXP(0.014393/(cw1*Thstart))-1.)	Convert Th to band 1 spectral radiant exitance (Rh1 in $W m^{-2} m^{-1}$)
Rhstart2 = 0.00000000000000003741*cw2^(-5./ (EXP(0.014393/(cw2*Thstart))-1.)	Convert Th to band 2 spectral radiant exitance (Rh2 in $W m^{-2} m^{-1}$)
p1 = (R1-Rc1)/(Rhstart1-Rc1)	Calculate pixel portion occupied by hot component in band 1 (p1)
p2 = (R2-Rc2)/(Rhstart2-Rc2)	Calculate pixel portion occupied by hot component in band 2 (p2)
Ratio = p1/p2	Calculate ratio of p1/p2 (Ratio)
Th = Thstart	Set Th at start of iteration loop
LOOP	
WHILE (Ratio NE 1.0) DO BEGIN	Loop until p1/p2 = 1 (i.e., p1 = p2)
IF (Ratio GT 1.0) THEN Th = Th + 0.1 ELSE Th = Th - 0.1	If p1 > p2, then we increase Th, otherwise if p1 < p2, then we decrease Th

Table S6.1. (cont.)

Code	Comment
$Rh1 = 0.0000000000000003741 * cw1^{(-5.)} / (EXP(0.014393/(cw1 * Th)) - 1.)$	Convert T_h to band 1 spectral radiant exitance (Rh1 in $W m^{-2} m^{-1}$)
$Rh2 = 0.0000000000000003741 * cw2^{(-5.)} / (EXP(0.014393/(cw2 * Th)) - 1.)$	Convert T_h to band 2 spectral radiant exitance (Rh2 in $W m^{-2} m^{-1}$)
$p1 = (R1 - Rc1) / (Rh1 - Rc1)$	Calculate pixel portion occupied by hot component in band 1 (p1)
$p2 = (R2 - Rc2) / (Rh2 - Rc2)$	Calculate pixel portion occupied by hot component in band 2 (p2)
Ratio = p1/p2	Calculate ratio of p1/p2 (Ratio)
IF (Ratio GT 0.999) AND (Ratio LT 1.001) THEN Ratio = 1.0 ELSE Ratio=Ratio	Condition to stop the loop once the ratio is within 3 decimal places of 1.0
ENDWHILE	End loop if condition is met (i.e., p1/p2 = 1 so that p1 = p2)
OUTPUT	
$Th1 = 0.014393 / (cw1 * alog((0.0000000000000003741 * cw1^{(-5.)} / Rh1) + 1))$	Convert output band 1 hot spot radiance to a temperature (T_h , K)
$Th2 = 0.014393 / (cw2 * alog((0.0000000000000003741 * cw2^{(-5.)} / Rh2) + 1))$	Convert output band 2 hot spot radiance to a temperature (T_h , K)
Print, "Input Band 1 Temperature (K) = ", BT1	Print input band 1 pixel-integrated temperature (Kelvin)
Print, "Input Band 2 Temperature (K) = ", BT2	Print input band 2 pixel-integrated temperature (Kelvin)
Print, "Assumed Cool Component Temperature (K) = ", Tc	Print assumed cold component temperature (Kelvin)
Print, "Solved T_h in Bands 1 and 2 (K) = ", Th1, Th2	Print solution for hot component temperature in bands 1 and 2 (Kelvin)*
Print, "Solved p in Bands 1 and 2 = ", p1, p2	Print solution for hot component portion in bands 1 and 2
Print, "Ratio of p1/p2 = ", Ratio	Print p1/p2 ration (this should equal 1.0 if a solution has been reached)
END	End program

* Note, for a good solution T_{h1} and T_{h2} must be the same, thus we print these both out to allow a check. The same applies to p.

In both cases, solution will occur when T_c in waveband 1 is the same as T_c in waveband 2. Numerically, the approach is the same as solving when T_c is known (i.e., the solution of Chapter 4, Section 4.2.1.1), where we adjust either p or T_h in a positive or negative direction depending on whether we are moving towards or away from the solution point defined by the condition $T_c(\lambda_1) = T_c(\lambda_2)$.

(i) Solution by assuming T_h

For this option we assume T_h and adjust p until $T_c(\lambda_1) = T_c(\lambda_2)$. If, for example, we have a vent temperature measurement of 950 °C, we can convert this to a spectral radiant exitance in the MIR ($= \lambda_1$) of $2.29 \times 10^{10} \text{ W m}^{-2} \text{ m}^{-1}$ and of $1.21 \times 10^9 \text{ W m}^{-2} \text{ m}^{-1}$ in the TIR ($= \lambda_2$). For the hot spot scenario Section 4.1.1.3 of Chapter 4 we have pixel-integrated temperatures of 248 °C in the MIR and 58 °C in the TIR, which convert to spectral radiant exitances of $3.21 \times 10^8 \text{ W m}^{-2} \text{ m}^{-1}$ and $4.57 \times 10^7 \text{ W m}^{-2} \text{ m}^{-1}$. If we start with p of 0.001, and input these spectral radiant exitances into Equations (S6.2a) and (S6.2b) we obtain

$$M(\lambda_1, T_c) = \frac{3.21 \times 10^8 \text{ W m}^{-2} \text{ m}^{-1} - 0.001(2.29 \times 10^{10} \text{ W m}^{-2} \text{ m}^{-1})}{(1 - 0.001)} = 2.98 \times 10^8 \text{ W m}^{-2} \text{ m}^{-1}$$

$$M(\lambda_2 T_c) = \frac{4.57 \times 10^7 \text{ W m}^{-2} \text{ m}^{-1} - 0.001(1.21 \times 10^9 \text{ W m}^{-2} \text{ m}^{-1})}{(1 - 0.001)} = 4.46 \times 10^7 \text{ W m}^{-2} \text{ m}^{-1}$$

This converts to $T_c(\lambda_1) = 243$ °C and $T_c(\lambda_2) = 56$ °C. Hence, $T_c(\lambda_1)$ is greater than $T_c(\lambda_2)$, so this is not the solution. Thus we increase p . If we increase p to 0.01 we now have

$$M(\lambda_1, T_c) = \frac{3.21 \times 10^8 \text{ W m}^{-2} \text{ m}^{-1} - 0.01(2.29 \times 10^{10} \text{ W m}^{-2} \text{ m}^{-1})}{(1 - 0.01)} = 9.28 \times 10^7 \text{ W m}^{-2} \text{ m}^{-1}$$

$$M(\lambda_2 T_c) = \frac{4.57 \times 10^7 \text{ W m}^{-2} \text{ m}^{-1} - 0.01(1.21 \times 10^9 \text{ W m}^{-2} \text{ m}^{-1})}{(1 - 0.01)} = 3.39 \times 10^7 \text{ W m}^{-2} \text{ m}^{-1}$$

This converts to $T_c(\lambda_1) = 173$ °C and $T_c(\lambda_2) = 35$ °C. By increasing p while holding T_h constant, we have had to decrease the cool component temperature to maintain the values of T_{int} in the two wavebands. However, T_c in waveband λ_1 is still greater than T_c in waveband λ_2 . Thus we continue to increase p until we arrive at:

$$M(\lambda_1, T_c) = \frac{3.21 \times 10^8 \text{ W m}^{-2} \text{ m}^{-1} - 0.0139626(2.29 \times 10^{10} \text{ W m}^{-2} \text{ m}^{-1})}{(1 - 0.0139626)} \\ = 1.29 \times 10^6 \text{ W m}^{-2} \text{ m}^{-1}$$

$$M(\lambda_2 T_c) = \frac{4.57 \times 10^7 \text{ W m}^{-2} \text{ m}^{-1} - 0.0139626(1.21 \times 10^9 \text{ W m}^{-2} \text{ m}^{-1})}{(1 - 0.0139626)} = 2.92 \times 10^7 \text{ W m}^{-2} \text{ m}^{-1}$$

These spectral radiant exitances convert to T_c of 25 °C in both wavebands, with solution occurring at $p \sim 0.014$, i.e., the model input parameters.

By way of a worked example, a piece of code that applies the dual-band method to solve for p and T_c by assuming T_h and iterating on p is given in Table S6.2. Note that, if we input a

Table S6.2. (cont.)

Code	Comment
Tc1 = 0.014393/(cw1*log ((0.0000000000000003741* cw1 ^(-5.) /Rc1)+1))	Convert starting band 1 cold component radiance to a temperature (Tc, K)
Tc2 = 0.014393/(cw2*log ((0.0000000000000003741* cw2 ^(-5.) /Rc2)+1))	Convert starting band 2 cold component radiance to a temperature (Tc, K)
Diff = Tc1-Tc2	Calculate the difference in temperature between Tc1 and Tc2 (Diff, K)
LOOP	
WHILE (Diff NE 0.0) DO BEGIN	Loop until Tc1-Tc2 = 0.0 (i.e., Tc1 = Tc2)
IF (Tc1 GT Tc2) THEN p = p + 0.0000001	If Tc1 > Tc2, then we increase p, otherwise if
ELSE p = p - 0.0000001	Tc1 < Tc2, then we decrease p
Rc1 = (R1 - p*Rh1)/(1-p)	Calculate radiance of cold component in band 1 (Rc1)
Rc2 = (R2 - p*Rh2)/(1-p)	Calculate radiance of cold component in band 2 (Rc2)
Tc1 = 0.014393/(cw1*log ((0.0000000000000003741* cw1 ^(-5.) /Rc1)+1))	Convert starting band 1 cold component radiance to a temperature (Tc, K)
Tc2 = 0.014393/(cw2*log ((0.0000000000000003741* cw2 ^(-5.) /Rc2)+1))	Convert starting band 2 cold component radiance to a temperature (Tc, K)
Diff = Tc1-Tc2	Calculate the difference in temperature between Tc1 and Tc2 (Diff, K)
IF (Diff GT -1.000) AND (Diff LT 1.000) THEN	Condition to stop the loop once the difference is within 1 degree of 0.0
Diff = 0.0 ELSE Diff=Diff	
ENDWHILE	End loop if condition is met (i.e., Tc1-Tc2 = 0 so that Tc1 = Tc2)
OUTPUT	
Print, "Input Band 1 Temperature (K) = ", BT1	Print input band 1 pixel-integrated temperature (Kelvin)
Print, "Input Band 2 Temperature (K) = ", BT2	Print input band 2 pixel-integrated temperature (Kelvin)
Print, "Assumed Hot Component Temperature (K) = ", Th	Print assumed hot component temperature (Kelvin)
Print, "Solved Tc in Bands 1 and 2 (K) = ", Tc1, Tc2	Print solution for cold component temperature in bands 1 and 2 (Kelvin)*
Print, "Solved p = ", p	Print solution for hot component portion
END	End program

* Note, for a good solution Tc1 and Tc2 must be the same, thus we print these both out to allow a check. The same applies to Th.

place a trap in the code to check for such a case. If this case is encountered, the starting p will have to be decreased until the spectral radiant exitances become positive. Also, rather than using the ratio of $T_c(\lambda_1)$ to $T_c(\lambda_2)$ I have used the difference, stopping the loop once the difference approaches zero.

(ii) Solution by assuming p

For this option, we assume p and adjust T_h until $T_c(\lambda_1) = T_c(\lambda_2)$. Take, for example, the case where we can measure the vent radius ($r = 2$ m) so that we know the vent area ($A = \pi r^2 = 12.57$ m²) and pixel area ($TM = 900$ m²). We thus know that the pixel portion occupied by the vent is

$$p = 12.57 \text{ m}^2 / 900 \text{ m}^2 = 0.013963$$

If we start with a T_h of 1200 °C, we find that the radiance in the MIR has to be negative in order to solve,

$$M(\lambda_1, T_c) = \frac{3.21 \times 10^8 \text{ Wm}^{-2} \text{ m}^{-1} - 0.014(4.02 \times 10^{10} \text{ Wm}^{-2} \text{ m}^{-1})}{(1 - 0.014)} = -2.45 \times 10^8 \text{ Wm}^{-2} \text{ m}^{-1}$$

A negative radiance cannot be converted to a pixel-integrated temperature so we reject this solution, and instead start with a T_h that is equal to 25 °C. For this combination of T_h and p we have:

$$M(\lambda_1, T_c) = \frac{3.21 \times 10^8 \text{ Wm}^{-2} \text{ m}^{-1} - 0.014(1.29 \times 10^6 \text{ Wm}^{-2} \text{ m}^{-1})}{(1 - 0.014)} = 3.25 \times 10^8 \text{ Wm}^{-2} \text{ m}^{-1}$$

$$M(\lambda_2 T_c) = \frac{4.57 \times 10^7 \text{ Wm}^{-2} \text{ m}^{-1} - 0.014(2.92 \times 10^7 \text{ Wm}^{-2} \text{ m}^{-1})}{(1 - 0.014)} = 4.06 \times 10^7 \text{ Wm}^{-2} \text{ m}^{-1}$$

This converts to $T_c(\lambda_1) = 249$ °C and $T_c(\lambda_1) = 59$ °C. Hence, $T_c(\lambda_1)$ is greater than $T_c(\lambda_2)$. We also note that the cold component temperature is higher than that of the assumed hot component (25 °C). Thus we increase T_h . If we increase T_h to 500 °C, we now have

$$M(\lambda_1, T_c) = \frac{3.21 \times 10^8 \text{ Wm}^{-2} \text{ m}^{-1} - 0.014(3.55 \times 10^9 \text{ Wm}^{-2} \text{ m}^{-1})}{(1 - 0.014)} = 2.75 \times 10^8 \text{ Wm}^{-2} \text{ m}^{-1}$$

$$M(\lambda_2 T_c) = \frac{4.57 \times 10^7 \text{ Wm}^{-2} \text{ m}^{-1} - 0.014(5.24 \times 10^8 \text{ Wm}^{-2} \text{ m}^{-1})}{(1 - 0.014)} = 3.09 \times 10^7 \text{ Wm}^{-2} \text{ m}^{-1}$$

This converts to $T_c(\lambda_1) = 238$ °C and $T_c(\lambda_2) = 46$ °C. T_c in waveband λ_1 is still greater than T_c in waveband λ_2 . Thus we continue to increase T_h until we arrive at:

$$M(\lambda_1, T_c) = \frac{3.21 \times 10^8 \text{ Wm}^{-2} \text{ m}^{-1} - 0.014(2.29 \times 10^{10} \text{ Wm}^{-2} \text{ m}^{-1})}{(1 - 0.014)} = 1.29 \times 10^6 \text{ Wm}^{-2} \text{ m}^{-1}$$

$$M(\lambda_2, T_c) = \frac{4.57 \times 10^7 \text{ Wm}^{-2} \text{ m}^{-1} - 0.014(1.21 \times 10^9 \text{ Wm}^{-2} \text{ m}^{-1})}{(1 - 0.014)} = 2.29 \times 10^7 \text{ Wm}^{-2} \text{ m}^{-1}$$

These spectral radiant exitances convert to T_c of 25 °C in both wavebands, with solution occurring at T_h of 950 °C, i.e., the model input parameters. By way of a worked example, a piece of code that applies the dual-band method to solve for T_h and T_c by assuming p and iterating on T_h is given in Table S6.3.

Reality

I have kept the cases worked-up so far generic by using a simple model-based numeric example. This keeps things simple for purposes of demonstrating how the methodologies work. However, in reality, things are a little more complicated and problems are induced by non-detection and/or saturation. Thus, methodologies have to be selected depending on the limits of the data (in terms of non-detection and/or saturation), available wavebands, and the type of hot spot likely present within the pixel (one-, two-, or three-component). These issues differ depending on whether AVHRR- or TM-class data are being used.

Application to AVHRR-class data

Given the conditions required for the two-component dual-band method to work, it applies best to situations where a single, isothermal hot spot is present in a pixel against a cooler, isothermal background. For AVHRR-class pixels this may apply to a case where a single hot vent is present against a cold ambient background, as envisaged for our test-case scenario. However, the hot spot needs to be large enough and hot enough to provide an anomaly in the thermal infrared, but not so large that it saturates the mid-infrared.

Case 1: Two-components, no-response in the TIR

In Figure S6.1 I give the temperature grid obtained from an AVHRR image of Mount Etna. This grid is centered on Etna's summit craters and is of pixel-integrated temperatures corrected for atmospheric effects, as well as for surface reflection and emissivity effects, in AVHRR bands 3, 4 and 5.

In Section 4.1.1.2 of Chapter 4 we used this grid to test the application of the two-component mixture model of Marsh (1980) to the TIR. For this test, one band of TIR data (AVHRR band 4 or 5) was shown capable of extracting the sub-pixel area of a snow patch

AVHRR Band 3

39.5	37.7	29.2	16.8
35.4	34.3	32.0	20.5
34.6	32.8	28.8	24.5

AVHRR Band 4

39.7	35.8	27.0	22.7
37.6	34.9	29.0	26.2
36.8	35.5	33.3	29.7

AVHRR Band 5

39.8	36.4	26.9	22.1
37.5	34.9	29.5	25.7
36.4	35.0	32.2	29.7

KEY

34.3	Ground-truth pixel containing snow and scoria
32.0	Summit pixel containing active vent
35.4	Other (ambient) pixel

Figure S6.1 AVHRR bands 3, 4 and 5 pixel grids, centered on Mount Etna's summit, extracted from an image acquired on 3 June 1994 at 15:06Z. Values are pixel-integrated temperatures in °C.

For this scenario, we can assume a two-component mixture model (i.e., hot vent surrounded by cold ground) and apply the two-component dual-band method Section 4.2.1 (Chapter 4). However, because we have an anomaly in only one waveband, we can only use one waveband of data. As explained in Section 4.2.1.3 (Chapter 4), we can use the non-response of the TIR to our advantage. We thus apply the two-component, single band solution of Section 4.2.1.3 to estimate the vent area. This solution assumes no hot spot contribution to the integrated radiance in the TIR and uses the TIR pixel-integrated temperature to set the background temperature – in this case the temperature of ambient surfaces surrounding the vent, i.e., T_c in Equation (S6.1a). Now, using the field-measured temperature of the vent (340 °C, using a Minolta/Land Compac 3 radiometer) with the AVHRR band 5 pixel integrated temperature for this pixel (29.5 °C) we can solve to estimate the pixel portion occupied by the hot vent (p):

$$p = \frac{M(\lambda_{MIR}, T_{int}) - M(\lambda_{MIR}, T_c)}{M(\lambda_{MIR}, T_h) - M(\lambda_{MIR}, T_c)} = \frac{M(3.74\mu m, 32.0^\circ C) - M(3.74\mu m, 29.5^\circ C)}{M(3.74\mu m, 340^\circ C) - M(3.74\mu m, 29.5^\circ C)}$$

$$= \frac{1.70 \times 10^6 \text{ Wm}^{-2} \text{m}^{-1} - 1.53 \times 10^6 \text{ Wm}^{-2} \text{m}^{-1}}{9.63 \times 10^8 \text{ Wm}^{-2} \text{m}^{-1} - 1.53 \times 10^6 \text{ Wm}^{-2} \text{m}^{-1}} = 0.000177$$

Thus, the hot vent occupies 0.000177 or 0.0177 % of the pixel. Given that the pixel area for this image was 2.016 km², this gives a vent area of 0.000177 × 2016039 m² = 358 m². This is

equivalent to a ~19 m diameter circular vent, and squares perfectly with the presence of two 10 m wide degassing vents observed at Etna's summit during the time of the satellite overpass.

Case 2: Two components, two bands

In Table S6.4 we the AVHRR band 3 and 4 pixel-integrated temperatures for the hot pixel containing the active lava lake at Mount Erebus in seven images acquired in 1980. We see that, for three cases, we have unsaturated data in bands 3 and 4. Thus for these pixels we make the assumption that the pixel is occupied by a hot volcanic (lava lake) source surrounded by a very cold (icy) ambient background. We see that the size of the hot spot is so small, and the background so cold, that the "hot" pixel in band 4 is around minus 20 °C; however this is still typically between 3 °C and 10 °C hotter than the background (ice-filled) pixels.

We now estimate the background temperature using the average pixel-integrated temperature for the four band 4 pixels immediately adjacent to the hot spot pixel in each of the cardinal directions. This value is given as T_b in Table S6.4. This allows us solve the two-component dual-band system using two bands of data following the method given above, where we assume the background (ambient) value and solve for p by iterating T_h . That is, for the 10 February 1980 image, we insert our values into the simultaneous Equations of (S6.1), i.e.,

$$M(3.74\mu\text{m}, 44.7\text{ }^\circ\text{C}) = p M(3.74\mu\text{m}, T_h) + (1-p) M(3.74\ \mu\text{m}, -26.6\text{ }^\circ\text{C})$$

$$M(10.8\mu\text{m}, -23.4\text{ }^\circ\text{C}) = p M(10.8\mu\text{m}, T_h) + (1-p) M(10.8\ \mu\text{m}, -26.6\text{ }^\circ\text{C})$$

Written in terms of radiance, and rearranged, we have:

$$p_{\lambda 3} = \frac{(1.27\text{mWsr}^{-1}\text{m}^{-2}\text{cm}^{-1}) - (0.0385\text{mWsr}^{-1}\text{m}^{-2}\text{cm}^{-1})}{M(\lambda_3, T_h) - (0.0385\text{mWsr}^{-1}\text{m}^{-2}\text{cm}^{-1})}$$

$$p_{\lambda 4} = \frac{(45.6\text{mWsr}^{-1}\text{m}^{-2}\text{cm}^{-1}) - (45.5\text{mWsr}^{-1}\text{m}^{-2}\text{cm}^{-1})}{M(\lambda_4, T_h) - (45.5\text{mWsr}^{-1}\text{m}^{-2}\text{cm}^{-1})}$$

If we start with a T_h of 0 °C, we obtain

$$p_{\lambda 3} = \frac{(1.27\text{mWsr}^{-1}\text{m}^{-2}\text{cm}^{-1}) - (0.0385\text{mWsr}^{-1}\text{m}^{-2}\text{cm}^{-1})}{(0.1757\text{mWsr}^{-1}\text{m}^{-2}\text{cm}^{-1}) - (0.0385\text{mWsr}^{-1}\text{m}^{-2}\text{cm}^{-1})} = 9$$

$$p_{\lambda 4} = \frac{(45.6\text{mWsr}^{-1}\text{m}^{-2}\text{cm}^{-1}) - (45.5\text{mWsr}^{-1}\text{m}^{-2}\text{cm}^{-1})}{(9.0\text{mWsr}^{-1}\text{m}^{-2}\text{cm}^{-1}) - (45.5\text{mWsr}^{-1}\text{m}^{-2}\text{cm}^{-1})} = 0.1$$

Thus, $p_{\lambda 3}$ is greater than $p_{\lambda 4}$ (and is also greater than one), so solution has not been reached. We thus increase T_c , following the procedure laid out above, until we reach a solution

Table S6.4 AVHRR band 3 and 4 pixel-integrated temperatures (T_3 and T_4) and background values (T_w), corrected for atmospheric effects and emissivity, for anomalous AVHRR pixels containing an active lava lake at Erebus during 1980. The pixel portion occupied by lava, and the lava area that this converts to, are given for two methodologies: (1) the dual-band method if bands 3 and 4 are unsaturated, and (2) the two-component, one-band TIR method (using three assumed lava surface, T_c , temperatures) if band 3 is saturated. Method 1 gives plausible results (i.e., a reasonable temperature and a lake area that compares with the field measured value of $\sim 2800 \text{ m}^2$) for the 10 February image. For the other two images to which this method is applied, the first gives a lake area that appears a little too large, the second gives no solution (the image may be contaminated by high cloud). Method 2 gives reasonable values for all images (including the 13 January 1980 image that gives unrealistic values when method 1 is applied) for the $580 \text{ }^\circ\text{C}$ and $715 \text{ }^\circ\text{C}$ T_c temperature assumptions. Output always need to be assessed against field data to assess the realism of the result; unrealistic results suggest an assumption required to apply a given dual-band solution model is invalid.

Date	Time (UT)	Scan Angle (degrees)	Pixel Area (km^2)	T_3 ($^\circ\text{C}$)	T_4 ($^\circ\text{C}$)	T_b ($^\circ\text{C}$)	Method	Solution
12-Jan-80	15:14	24.0	1.549	Saturated	-21.0	-25.8	Two-component, TIR one band	$T_c = 360 \text{ }^\circ\text{C}$, $p = 0.0037$, $A = 5700 \text{ m}^2$ $T_c = 580 \text{ }^\circ\text{C}$, $p = 0.0019$, $A = 2950 \text{ m}^2$ $T_c = 715 \text{ }^\circ\text{C}$, $p = 0.0014$, $A = 2200 \text{ m}^2$
13-Jan-80	9:53	25.0	1.595	44.1	-19.0	-23.7	Dual-band: Two bands, two components	Solved $T_c = 284 \text{ }^\circ\text{C}$ Solve $p = 0.0052$ Lake Area = 8300 m^2
							Two-component, TIR one band	$T_c = 360 \text{ }^\circ\text{C}$, $p = 0.0037$, $A = 5950 \text{ m}^2$ $T_c = 580 \text{ }^\circ\text{C}$, $p = 0.0019$, $A = 30950 \text{ m}^2$ $T_c = 715 \text{ }^\circ\text{C}$, $p = 0.0014$, $A = 2300 \text{ m}^2$
13-Jan-80	11:34	5.5	1.137	Saturated	-21.8	-24.4	Two-component, TIR one band	$T_c = 360 \text{ }^\circ\text{C}$, $p = 0.0020$, $A = 2300 \text{ m}^2$ $T_c = 580 \text{ }^\circ\text{C}$, $p = 0.0010$, $A = 1200 \text{ m}^2$ $T_c = 715 \text{ }^\circ\text{C}$, $p = 0.0008$, $A = 900 \text{ m}^2$
13-Jan-80	16:32	13.0	1.227	Saturated	-14.9	-22.5	Two-component, TIR one band	$T_c = 360 \text{ }^\circ\text{C}$, $p = 0.0063$, $A = 7700 \text{ m}^2$ $T_c = 580 \text{ }^\circ\text{C}$, $p = 0.0032$, $A = 3900 \text{ m}^2$ $T_c = 715 \text{ }^\circ\text{C}$, $p = 0.0024$, $A = 2700 \text{ m}^2$

Table S6.4 (cont.)

Date	Time (UT)	Scan Angle (degrees)	Pixel Area (km ²)	T ₃ (°C)	T ₄ (°C)	T _b (°C)	Method	Solution
10-Feb-80	18:08	12.6	1.220	44.7	-23.4	-26.6	Dual-band: Two bands, two components	Solved T _c = 355 °C Solve p = 0.0025 Lake Area = 3000 m ²
7-Nov-80	15:30	23.8	1.540	30.3	-33.5	-35.2	Dual-band: Two bands, two components	No solution
29-Nov-80	7:50	9.1	1.170	Saturated	-19.4	-29.1	Two-component, TIR one band	T _c = 360 °C, p = 0.0074, A = 8600 m ² T _c = 580 °C, p = 0.0038, A = 4450 m ² T _c = 715 °C, p = 0.0029, A = 3350 m ²

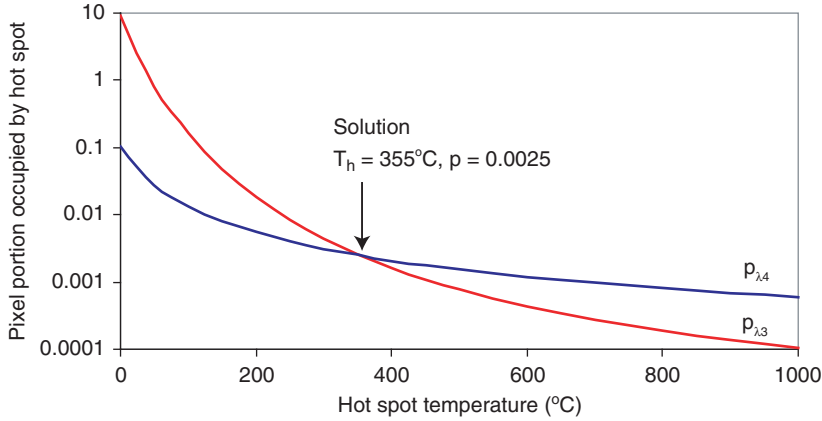


Figure S6.2 Dual-band solution for an AVHRR pixel at Mount Erebus with a band 3 pixel-integrated temperature of 44.7°C and a band 4 pixel-integrated temperature of -23.4°C . Assumed background temperature is -26.6°C . Image was acquired on 10 February 1980.

(i.e., $p_{\lambda 3} = p_{\lambda 4}$). This occurs at a p of 0.0025 and a hot component temperature of 355°C , with the graphical solution being given in Figure S6.2. If we multiply p by the pixel area (1.22 km^2) we obtain a lava lake area of $\sim 3000\text{ m}^2$. This compares with a lake area obtained from air photographs acquired during the same year of 2800 m^2 .

Case 3: Two-components, one band

If the hot spot is of sufficient size and/or temperature to create an anomaly in AVHRR band 4, more often than not it will also be of sufficient size or temperature to saturate band 3. We see this effect in Table S6.4, in which we have saturated data in four of the seven cases. For these cases, we thus have to resort to a two-component, single-band solution that uses the TIR, i.e., the solution of Section 4.2.1.4 (Chapter 4). Take the data acquired on 13 January 1980 at 11:34Z. Using the band 4 pixel-integrated temperature for the lava lake pixel, setting the background temperature as in the previous case and assuming the hot spot temperature also obtained in the previous case, we obtain:

$$M(10.8\mu\text{m}, -21.8^\circ\text{C}) = p M(10.8\mu\text{m}, 360^\circ\text{C}) + (1-p)M(10.8\mu\text{m}, -24.4^\circ\text{C})$$

Now converting the spectral radiance and rearranging gives solution for p :

$$p_{\lambda 4} = \frac{(47.2\text{mWsr}^{-1}\text{m}^{-2}\text{cm}^{-1}) - (44.6\text{mWsr}^{-1}\text{m}^{-2}\text{cm}^{-1})}{(1315\text{mWsr}^{-1}\text{m}^{-2}\text{cm}^{-1}) - (44.6\text{mWsr}^{-1}\text{m}^{-2}\text{cm}^{-1})} = 0.002$$

This solution will have to be consistent with saturation of band 3, which we can check by inserting the values into the mixture model for the predicted band 3 pixel-integrated radiance:

$$M(3.74\mu\text{m}, T_{\text{int}}) = 0.002M(3.74\mu\text{m}, 360^\circ\text{C}) + (1-0.002)M(3.74\mu\text{m}, -24.4^\circ\text{C})$$

This gives a pixel-integrated radiance of $1.1 \text{ mW sr}^{-1} \text{ m}^{-2} \text{ cm}^{-1}$ which converts to a pixel-integrated temperature of $\sim 40^\circ\text{C}$. This is $\sim 10^\circ\text{C}$ lower than the typical saturation temperature for AVHRR band 3, and so is not consistent with saturation.

The solution of Harris *et al.* (1999) instead used the typical hot spot temperature range obtained from a January 1989 TM image of the Erebus lava lake which gave typical lake surface temperatures of 580°C to 715°C . Using these now yields;

$$M(10.8\mu\text{m}, -21.8^\circ\text{C}) = p M(10.8\mu\text{m}, 580^\circ\text{C}) + (1-p) M(10.8\mu\text{m}, -24.4^\circ\text{C})$$

and

$$M(10.8\mu\text{m}, -21.8^\circ\text{C}) = p M(10.8\mu\text{m}, 715^\circ\text{C}) + (1-p) M(10.8\mu\text{m}, -24.4^\circ\text{C})$$

Which gives

$$p_{\lambda 4} = \frac{(47.2 \text{ mWsr}^{-1} \text{ m}^{-2} \text{ cm}^{-1}) - (44.6 \text{ mWsr}^{-1} \text{ m}^{-2} \text{ cm}^{-1})}{(2516 \text{ mWsr}^{-1} \text{ m}^{-2} \text{ cm}^{-1}) - (44.6 \text{ mWsr}^{-1} \text{ m}^{-2} \text{ cm}^{-1})} = 0.001$$

and

$$p_{\lambda 4} = \frac{(47.2 \text{ mWsr}^{-1} \text{ m}^{-2} \text{ cm}^{-1}) - (44.6 \text{ mWsr}^{-1} \text{ m}^{-2} \text{ cm}^{-1})}{(3325 \text{ mWsr}^{-1} \text{ m}^{-2} \text{ cm}^{-1}) - (44.6 \text{ mWsr}^{-1} \text{ m}^{-2} \text{ cm}^{-1})} = 0.0008$$

Given the $\sim 1.14 \text{ km}^2$ pixel area, this is equivalent to a lava lake area (A_{lake}) of between

$$A_{\text{lake}} = 0.001 \times 1137000 \text{ m}^2 = 1140 \text{ m}^2$$

and

$$A_{\text{lake}} = 0.0008 \times 1137000 \text{ m}^2 = 920 \text{ m}^2$$

The two solutions also yield equivalent pixel-integrated temperatures in band 3 of 86°C and 108°C , which meet the band 3 saturation condition. Other solutions achieved in this manner for this data set, as listed in Table S6.4, yield a typical lake area of between 2200 m^2 and 4500 m^2 (mean = 2700 m^2), consistent with the field measurement of $\sim 2800 \text{ m}^2$.

Case 3: Three components, saturation in the MIR

Over an active lava, one to four kilometer AVHRR- and GOES-class pixels will likely have a three component structure, comprising:

- (i) crusted lava, containing
- (ii) hot cracks, surrounded by
- (iii) cold, lava-free ground.

The three-component approach of Section 4.3.1.1 of Chapter 4 thus needs to be applied to such a pixel. However, more often than not, AVHRR data acquired over an active lava flow is also saturated in the MIR, so that only one band of TIR data is available. The lower sensitivity of AVHRR TIR band (band 4) means that these data are often below saturation so that, if we can make the assumption that the cracks do not contribute to the integrated radiance in band 4, we can apply the one-band, two-component TIR solution of Section 4.3.1.2 (Chapter 4) to determine the lava area.

Following this method, the typical lava surface temperature (T_c) and background temperatures (T_a) are assumed, and used with the TIR pixel integrated temperature (T_{int}) to solve for the pixel portion occupied by the hot lava source (p) in

$$p = \frac{M(\lambda_{TIR}, T_{\text{int}}) - M(\lambda_{TIR}, T_a)}{M(\lambda_{TIR}, T_c) - M(\lambda_{TIR}, T_a)} \quad (\text{S6.3})$$

In the example given in Table S6.5 we have the AVHRR band 4 pixel data for all radiant pixels containing an active lava flow field at Mount Etna during 17 and 18 November 2006. Three cloud-free images were available between 01:07Z on 17 November and 20:33Z on 18 November on which the presence of active lava caused between four and six band 4 pixels to become thermally anomalous. To apply the method to these pixels we complete the following steps:

- (i) Extract the pixel-integrated brightness temperatures (T_4) for each anomalous band 4 pixel.
- (ii) Take the minimum brightness temperature from all non-anomalous pixels surrounding the hot spot pixels, and use this for the assumed background temperature (T_a).
- (iii) Complete the necessary atmospheric and emissivity corrections. The corrected values for T_4 and T_a appearing in columns 1 and 2 of Table S6.5.
- (iv) Enter the assumed temperatures for the lava surface (T_c), convert all values (T_4 , T_a and T_c) to band 4 spectral radiances, and use these in the mixture model to solve for the pixel portion covered by lava at T_c (p). The result for each assumed T_c value, in this case 100, 250 and 600 °C, are given columns 3, 4 and 5 of Table S6.5.
- (v) Multiply by pixel area to obtain the lava area in each pixel (columns 6, 7 and 8 of Table S6.5).
- (vi) Sum the lava area for each pixel to obtain a total lava area for each image, as given at the base of each image block in Table S6.5.

The active lava area calculated for each T_c condition is consistent between each of the three images, but span a three order of magnitude range of between 0.0764 km² (for the $T_c = 100$ °C assumption) and 1.0828 km² (for the $T_c = 500$ °C assumption). However, this spans the measured area for lava flows active during 17–18 November 2006 (as obtained from LIDAR data) of 0.2827 km². The lava area ranges extracted for the $T_c = 250$ °C assumption (0.2726, 0.2670, and 0.2936 km²) are in excellent agreement with the measured value.

Table S6.5 Band 4 pixel-integrated temperatures (T_4) and background values (T_a), corrected for atmospheric effects and emissivity, for anomalous AVHRR pixels containing active lava acquired for Etna during 17–18 November 2006. The pixel portion occupied by lava calculated using Equation (S6.3) is given for three lava surface temperature (T_c) assumptions. This is multiplied by the pixel area (1.2144 km^2) to yield lava area for each pixel, and then summed for each image to give an estimate for total active lava area at each time.

Image data		Pixel Portion			Lava Area (km^2)		
T_4 ($^{\circ}\text{C}$)	T_a ($^{\circ}\text{C}$)	T_c , 100 $^{\circ}\text{C}$	T_c , 250 $^{\circ}\text{C}$	T_c , 600 $^{\circ}\text{C}$	T_c , 100 $^{\circ}\text{C}$	T_c , 250 $^{\circ}\text{C}$	T_c , 600 $^{\circ}\text{C}$
(1) Image: 17 November 2006 (01:07Z)							
5.3	-1.2	0.0427	0.0118	0.0034	0.0519	0.0143	0.0041
3.9	-1.2	0.0331	0.0091	0.0026	0.0402	0.0111	0.0032
10.4	-1.2	0.0780	0.0215	0.0062	0.0947	0.0262	0.0075
43.6	-1.2	0.3543	0.0978	0.0280	0.4303	0.1188	0.0340
28.8	-1.2	0.2215	0.0612	0.0175	0.2690	0.0743	0.0212
11.1	-1.2	0.0833	0.0230	0.0066	0.1012	0.0279	0.0080
Total for image		0.8130	0.2245	0.0642	0.9873	0.2726	0.0780
(2) Image: 17 November 2006 (20:46Z)							
8.7	-1.3	0.0663	0.0183	0.0052	0.0806	0.0223	0.0064
27.0	-1.3	0.2070	0.0572	0.0164	0.2514	0.0695	0.0199
10.5	-1.3	0.0790	0.0218	0.0062	0.0959	0.0265	0.0076
40.5	-1.3	0.3263	0.0902	0.0258	0.3963	0.1095	0.0313
15.7	-1.3	0.1171	0.0324	0.0093	0.1422	0.0393	0.0112
Total for image		0.7958	0.2198	0.0629	0.9664	0.2670	0.0764
(3) Image: 18 November 2006 (20:33Z)							
32.8	2.6	0.2375	0.0644	0.0183	0.2885	0.0782	0.0223
46.8	2.6	0.3700	0.1003	0.0286	0.4494	0.1219	0.0347
27.2	2.6	0.1886	0.0512	0.0146	0.2291	0.0621	0.0177
15.8	2.6	0.0955	0.0259	0.0074	0.1159	0.0314	0.0089
Total for image		0.8917	0.2418	0.0688	1.0828	0.2936	0.0836

Application to TM-class data

Application of the dual-band approach to TM and ETM+ data has been hindered by saturation problems, meaning that often only one band of useable data is available. In many cases, all data in all bands are often saturated. A variety of procedures applied to deal with such problems are detailed in Electronic Supplement 5. Here, we focus on two examples whereby data comprise (1) two bands of unsaturated and saturated pixels of identical spatial resolution, and (2) three bands of data which are unsaturated, but which are spread across wavebands with two different spatial resolutions.

Kilauea: two bands of saturated and unsaturated TM data

As described in Electronic Supplement 1, the size and temperature of most active lava bodies is such that emission often occurs in three TM bands (usually SWIR bands 5 and 7, plus TIR band 6), and sometimes also in a fourth (NIR band 4), over active lavas. The problem is, if we have a hot spot in band 5, the intensity of the emission required to achieve this often means that band 7 is saturated. Likewise presence of a hot spot in band 4 will often mean that both bands 5 and 7 are saturated. At the same time, the TIR band (band 6) is of a different spatial resolution to bands 4, 5 and 7 (120 m as opposed to 30 m). As a result, many variants of the dual-band method have been applied to TM data depending on (i) the assumptions regarding the hot spot emission properties and surface temperature that can be made, and (ii) the availability of responsive, unsaturated wavebands. These variants are detailed in Electronic Supplement 5. We here consider one of the solution options available, that applied by Flynn *et al.* (1994) to TM data for active pahoehoe at Kilauea. It is a solution set that covers most cases, i.e., it considers several possible combinations of responsive, non-responsive and saturated data.

Flynn *et al.*'s (1994) method first scanned the image to assess which pixels were anomalous in each band. To be anomalous, a DN in any band had to be elevated by five DN above a background level assigned for each band, and/or saturated. The radiances for all anomalous pixels were then extracted and corrected for reflection, atmospheric and emissivity effects. Finally, the *point-of-impossible-solution* test of Equation (4.11a) (Chapter 4) was applied to assess whether or not the dual band would solve or not. For the case of Flynn *et al.* (1994), where a hot component temperature of 1050 °C was assumed, the limit to the solution was given by

$$p_{\text{limit}} = M(\lambda, T_{\text{int}})/M(\lambda, T_{1050})$$

$M(\lambda, T_{1050})$ being the spectral radiance emitted at wavelength λ by a surface at 1050 °C. Thus, if p exceeded p_{limit} , a solution was rejected. Solving this equation shows that, for this case, p_{limit} is quite low. Take a pixel-integrated temperature of 200 °C in TM band 7, for example. For this value we have,

$$p_{\text{limit}} = (7.62 \times 10^6 \text{ W m}^{-2}\text{m}^{-1}) / (5.21 \times 10^{10} \text{ W m}^{-2}\text{m}^{-1}) = 1.46 \times 10^{-4},$$

that is, 0.01 % of a pixel.

The dual band method was then applied according to one of the following six cases:

CASE 1: *Unsaturated, anomalous data in bands 5 and 7, and pixel passes the point-of-impossible-solution test:*

Apply the dual band solution with the following form:

$$M(\lambda_5, T_{\text{int}}) = p M(\lambda_5, T_{\text{h}}) + (1-p) M(\lambda_5, T_{\text{c}})$$

$$M(\lambda_7, T_{\text{int}}) = p M(\lambda_7, T_{\text{h}}) + (1-p) M(\lambda_7, T_{\text{c}})$$

Assume a value (1150 °C) for the high temperature component (T_h), solve using the procedure outlined in 4.2.1. of Chapter 4 and output values for the crust temperature (T_c) and the fraction of each pixel occupied by crust.

CASE 2: *Unsaturated, anomalous data in both bands 5 and 7, but pixel fails the point-of-impossible-solution test:*

Pixel is assigned the band 7 pixel-integrated temperature. Band 7 is assumed to be primarily sensitive to the crust component, so that this value is assumed to equate to the crust temperature.

CASE 3: *Unsaturated, anomalous data in band 5, saturation of band 7:*

Pixel is assigned the band 5 pixel-integrated temperature.

CASE 4: *Saturated data in bands 5 and 7:*

Pixel is assigned the band 5 saturation temperature.

CASE 5: *No anomaly in band 5, but anomaly in band 7:*

Pixel is assigned the band 7 pixel-integrated temperature.

CASE 6: *No anomaly in bands 5 or 7, but anomaly in band 6:*

Pixel is assigned the band 6 pixel-integrated temperature.

Santiaguito: three bands of unsaturated data

Extrusion of silicic lava at Santiaguito was apparent from a thermal anomaly covering 26 band 6 (120 m) pixels on a 12 February 1993 Thematic Mapper image. Of these, only one was saturated. Within this larger anomaly were smaller band 5 and 7 anomalies, occupying 10 and 21 (30 m) pixels, respectively. Although four pixels were saturated in band 7, none were saturated in band 5. Although we have to accept that, for the saturated pixels, we only have a minimum value for the actual radiance, we can be happy that most pixels are unsaturated. We thus use these values in the radiance integration approach of Section 4.3.1.3 (Chapter 4) to integrate the bands 5, 6 and 7 spectral radiance across the entire band 6 anomaly, so that for this case, the integrated radiance in band 6 is obtained from (Equation 4.28, Chapter 4):

$$R_{6\ int} = \sum_{i=1}^n \left(\frac{120m \times 120m}{26 \times 120m \times 120m} R_{6i} \right) = \sum_{i=1}^n \left(\frac{14400m^2}{374400m^2} R_{6i} \right) = \sum_{i=1}^n \left(\frac{1}{26} R_{6i} \right)$$

and in bands 5 and 7 from,

$$R_{5,7\ int} = \sum_{i=1}^n \left(\frac{30m \times 30m}{26 \times 120m \times 120m} R_{5,7i} \right) = \sum_{i=1}^n \left(\frac{900m^2}{374400m^2} R_{5,7i} \right) = \sum_{i=1}^n \left(\frac{1}{416} R_{5,7i} \right)$$

The radiances for the band 6 pixels for this anomaly, all anomalous band 5 and 7 pixels within the band 6 anomaly area, and the weighted radiance values for each pixel, are given in Table S6.6, along with the three integrated radiances we obtain for this image.

Table S6.6 TM band 6, 7 and 5 pixel-integrated radiances and temperatures – corrected for atmospheric effects, reflection and emissivity - for anomalous pixels containing active lava acquired at Santiaguito on 12 February 1993. Bold values are saturated. The final three columns give the spectral radiance contribution for each pixel to the anomaly-integrated value, i.e., the pixel radiance weighted by the pixel area divided by the anomaly area. The final row in the table gives the summed contribution of each band, i.e., the anomaly-integrated radiance used to solve the three-component, three band problem.

Pixel-integrated spectral radiance (W m ⁻² m ⁻¹)			Pixel-integrated temperature (°C)			Total anomaly spectral radiance contribution (W m ⁻² m ⁻¹)		
Band 6	Band 7	Band 5	Band 6	Band 7	Band 5	Band 6	Band 7	Band 5
3.90E+07	1.01E+07	2.35E+07	48.5	211.8	346.2	1.50E+06	2.43E+04	5.64E+04
2.93E+07	4.48E+07	4.08E+07	26.9	272.1	371.4	1.13E+06	1.08E+05	9.80E+04
3.76E+07	4.52E+07	7.18E+07	45.6	272.4	399.5	1.45E+06	1.09E+05	1.73E+05
3.09E+07	1.74E+07	2.79E+07	30.7	232.1	353.9	1.19E+06	4.17E+04	6.71E+04
3.09E+07	9.39E+06	2.70E+07	30.7	209.2	352.4	1.19E+06	2.26E+04	6.50E+04
2.98E+07	4.52E+07	2.92E+07	28.0	272.4	356.0	1.14E+06	1.09E+05	7.03E+04
3.79E+07	4.52E+07	2.53E+07	46.1	272.4	349.4	1.46E+06	1.09E+05	6.07E+04
4.81E+07	4.52E+07	2.44E+07	66.3	272.4	347.8	1.85E+06	1.09E+05	5.86E+04
5.09E+07	2.39E+07	2.39E+07	71.5	245.0	347.0	1.96E+06	5.75E+04	5.75E+04
3.40E+07	2.18E+07	2.53E+07	37.8	241.2	349.4	1.31E+06	5.25E+04	6.07E+04
2.89E+07	3.97E+07		25.8	266.6		1.11E+06	9.53E+04	
4.19E+07	4.69E+07		54.4	274.2		1.61E+06	1.13E+05	
4.19E+07	3.64E+07		54.4	262.7		1.61E+06	8.74E+04	
3.38E+07	2.58E+07		37.3	248.1		1.30E+06	6.21E+04	
3.13E+07	2.58E+07		31.7	248.1		1.20E+06	6.21E+04	
3.22E+07	1.01E+07		33.8	211.8		1.24E+06	2.43E+04	
3.52E+07	1.67E+07		40.3	230.5		1.35E+06	4.01E+04	
3.18E+07	2.02E+07		32.7	238.1		1.22E+06	4.85E+04	
2.95E+07	2.07E+07		27.5	239.0		1.14E+06	4.96E+04	
3.04E+07	2.89E+07		29.6	252.8		1.17E+06	6.94E+04	
3.00E+07	1.43E+07		28.5	224.7		1.15E+06	3.44E+04	
2.98E+07			28.0			1.14E+06		
2.98E+07			28.0			1.14E+06		
2.89E+07			25.8			1.11E+06		
3.02E+07			29.1			1.16E+06		
2.91E+07			26.4			1.12E+06		
Σ						3.40E+07	1.43E+06	7.67E+05

The anomaly likely comprises a three-component structure comprising cool lava crust (at T_c) containing high temperature cracks (at T_h), surrounded by ambient ground (at T_a). We thus apply the *three bands of data, two assumptions* solution of Section 4.3.1.1 (Chapter 4), and use the anomaly-wide integrated spectral radiances of Table S6.6 in the following system of equations:

$$R_{6\text{int}} = p_a M(\lambda_6, T_a) + p_h M(\lambda_6, T_h) + (1 - p_a - p_h) M(\lambda_6, T_c)$$

$$R_{7\text{int}} = p_a M(\lambda_7, T_a) + p_h M(\lambda_7, T_h) + (1 - p_a - p_h) M(\lambda_7, T_c)$$

$$R_{5\text{int}} = p_a M(\lambda_5, T_a) + p_h M(\lambda_5, T_h) + (1 - p_a - p_h) M(\lambda_5, T_c)$$

By rearranging the first equation in the series, we can isolate p_a , so that

$$p_a = \frac{R_6 - M(\lambda_6, T_a) - p_h [M(\lambda_6, T_h) - M(\lambda_6, T_c)]}{M(\lambda_6, T_a) - M(\lambda_6, T_c)} = \beta_6$$

Inserting β_6 into the second and third equations in place of p_a gives,

$$R_{7\text{int}} = \beta_6 M(\lambda_7, T_a) + p_h M(\lambda_7, T_h) + (1 - \beta_6 - p_h) M(\lambda_7, T_c)$$

$$R_{5\text{int}} = \beta_6 M(\lambda_5, T_a) + p_h M(\lambda_5, T_h) + (1 - \beta_6 - p_h) M(\lambda_5, T_c)$$

Writing β_6 in full, rearranging and simplifying allows us now to write p_h in terms of T_c , T_h and T_a , i.e.,

$$p_{h7} = \frac{C_7 - [C_6 A_7]/A_6}{B_7 - [(B_6/A_6)A_7]}$$

$$p_{h5} = \frac{C_5 - [C_6 A_5]/A_6}{B_5 - [(B_6/A_6)A_5]}$$

in which

$$A_\lambda = M(\lambda, T_a) - M(\lambda, T_c)$$

$$B_\lambda = M(\lambda, T_a) - M(\lambda, T_c)$$

$$C_\lambda = R_{\lambda\text{int}} - M(\lambda, T_a)$$

This allows us to solve the equation system by assuming a hot component temperature ($T_h = 830$ °C) and obtaining a background temperature (T_a) from the mean of the lava-free band 6 pixels immediately surrounding the anomaly (for this case, this gives T_a of

16.2 °C). Now we can iterate on T_c until $p_{h7} = p_{h5}$. For example, if we start with a T_c of 100 °C, we obtain:

$$A_6 = (2.50 \times 10^7 \text{ W m}^{-2}\text{m}^{-1}) - (6.79 \times 10^7 \text{ W m}^{-2}\text{m}^{-1}) = -4.29 \times 10^7 \text{ W m}^{-2}\text{m}^{-1}$$

$$B_6 = (8.95 \times 10^8 \text{ W m}^{-2}\text{m}^{-1}) - (6.79 \times 10^7 \text{ W m}^{-2}\text{m}^{-1}) = 8.27 \times 10^8 \text{ W m}^{-2}\text{m}^{-1}$$

$$C_6 = (3.40 \times 10^7 \text{ W m}^{-2}\text{m}^{-1}) - (2.50 \times 10^7 \text{ W m}^{-2}\text{m}^{-1}) = 8.93 \times 10^6 \text{ W m}^{-2}\text{m}^{-1}$$

and

$$A_7 = (1.30 \times 10^3 \text{ W m}^{-2}\text{m}^{-1}) - (1.99 \times 10^5 \text{ W m}^{-2}\text{m}^{-1}) = -1.97 \times 10^7 \text{ W m}^{-2}\text{m}^{-1}$$

$$B_7 = (1.95 \times 10^{10} \text{ W m}^{-2}\text{m}^{-1}) - (1.99 \times 10^5 \text{ W m}^{-2}\text{m}^{-1}) = 1.95 \times 10^{10} \text{ W m}^{-2}\text{m}^{-1}$$

$$C_7 = (1.43 \times 10^6 \text{ W m}^{-2}\text{m}^{-1}) - (1.30 \times 10^3 \text{ W m}^{-2}\text{m}^{-1}) = 1.43 \times 10^6 \text{ W m}^{-2}\text{m}^{-1}$$

so that,

$$\frac{C_6 A_7}{A_6} = \frac{(8.93 \times 10^6 \text{ W m}^{-2}\text{m}^{-1})(-1.91 \times 10^5 \text{ W m}^{-2}\text{m}^{-1})}{-4.29 \times 10^7 \text{ W m}^{-2}\text{m}^{-1}} = 4.11 \times 10^4 \text{ W m}^{-2}\text{m}^{-1}$$

and

$$\frac{B_6}{A_6} A_7 = \frac{8.27 \times 10^8 \text{ W m}^{-2}\text{m}^{-1}}{-4.29 \times 10^7 \text{ W m}^{-2}\text{m}^{-1}} - 1.97 \times 10^5 \text{ W m}^{-2}\text{m}^{-1} = 3.81 \times 10^6 \text{ W m}^{-2}\text{m}^{-1}$$

giving,

$$p_{h7} = \frac{(1.43 \times 10^6 \text{ W m}^{-2}\text{m}^{-1}) - (4.11 \times 10^4 \text{ W m}^{-2}\text{m}^{-1})}{(1.95 \times 10^{10} \text{ W m}^{-2}\text{m}^{-1}) - (3.81 \times 10^6 \text{ W m}^{-2}\text{m}^{-1})} = 7.09 \times 10^{-5}$$

Likewise,

$$A_5 = (2.49 \times 10^0 \text{ W m}^{-2}\text{m}^{-1}) - (2.17 \times 10^3 \text{ W m}^{-2}\text{m}^{-1}) = -2.17 \times 10^3 \text{ W m}^{-2}\text{m}^{-1}$$

$$B_5 = (1.13 \times 10^{10} \text{ W m}^{-2}\text{m}^{-1}) - (2.17 \times 10^3 \text{ W m}^{-2}\text{m}^{-1}) = 1.13 \times 10^{10} \text{ W m}^{-2}\text{m}^{-1}$$

$$C_5 = (7.67 \times 10^5 \text{ W m}^{-2}\text{m}^{-1}) - (2.49 \times 10^0 \text{ W m}^{-2}\text{m}^{-1}) = -7.67 \times 10^5 \text{ W m}^{-2}\text{m}^{-1}$$

so that,

$$\frac{C_6 A_5}{A_6} = \frac{(8.93 \times 10^6 \text{ W m}^{-2}\text{m}^{-1})(-2.17 \times 10^3 \text{ W m}^{-2}\text{m}^{-1})}{-4.29 \times 10^7 \text{ W m}^{-2}\text{m}^{-1}} = 4.52 \times 10^2 \text{ W m}^{-2}\text{m}^{-1}$$

and

$$\frac{B_6}{A_6} A_5 = \frac{8.27 \times 10^8 \text{ W m}^{-2} \text{m}^{-1}}{-4.29 \times 10^7 \text{ W m}^{-2} \text{m}^{-1}} - 2.17 \times 10^3 \text{ W m}^{-2} \text{m}^{-1} = 4.19 \times 10^4 \text{ W m}^{-2} \text{m}^{-1}$$

giving,

$$p_{h5} = \frac{(7.67 \times 10^5 \text{ W m}^{-2} \text{m}^{-1}) - (4.52 \times 10^2 \text{ W m}^{-2} \text{m}^{-1})}{(1.13 \times 10^{10} \text{ W m}^{-2} \text{m}^{-1}) - (4.19 \times 10^4 \text{ W m}^{-2} \text{m}^{-1})} = 6.79 \times 10^{-5}$$

Clearly, this is not the solution, because p_{h7} is greater than p_{h5} ; so we increase T_c and test again until $p_{h7} = p_{h5}$, while ensuring that p_h , p_c and p_a are all positive and sum to one. The graphical solution for this case is given in Figure S6.3, and shows that solution occurs at p_h of 6.78×10^{-5} and T_c of 130°C . This can now be used with the band 6 radiances to calculate the p_c necessary to balance the Equation for Band 6, remembering that

$$p_a = \frac{R_6 - M(\lambda_6, T_a) - p_h[M(\lambda_6, T_h) - M(\lambda_6, T_c)]}{M(\lambda_6, T_a) - M(\lambda_6, T_c)}$$

so that

$$p_a = \frac{(3.40 \times 10^7 \text{ W m}^{-2} \text{m}^{-1}) - (2.50 \times 10^7 \text{ W m}^{-2} \text{m}^{-1}) - 6.78 \times 10^{-5} (8.27 \times 10^8 \text{ W m}^{-2} \text{m}^{-1})}{4.29 \times 10^7 \text{ W m}^{-2} \text{m}^{-1}} = 0.86$$

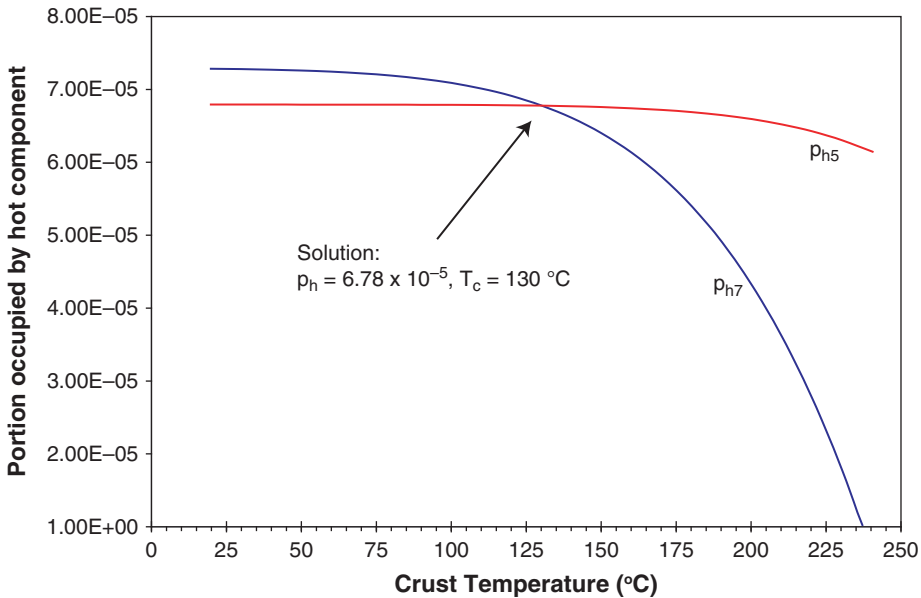


Figure S6.3 *Three bands of data, two assumptions* solution for the thermal anomaly at Santiaguito apparent in a 12 February 1993 TM image.

Thus the crusted lava component is calculated as occupying about 14 % of the 374 400 m² area of the thermal anomaly. The area occupied by the crusted lava can thus be obtained from

$$A_{\text{crust}} = (1 - 0.86) \times 374\,400 \text{ m}^2 = 52\,820 \text{ m}^2$$

to which the estimated area occupied by high temperature cracks,

$$A_{\text{crack}} = 6.78 \times 10^{-5} \times 374\,400 \text{ m}^2 = 25 \text{ m}^2$$

so that the lava area is

$$A_{\text{lava}} = A_{\text{crust}} + A_{\text{crack}} = 52\,820 \text{ m}^2 + 25 \text{ m}^2 = 52\,845 \text{ m}^2$$

The calculations suggest that we have a surface dominated by a chilled crust at a temperature of ~130 °C moving over ambient ground at ~16 °C, if the model is correct.

But is it Reality?

The short answer to the title of this section is, *we don't know*. A pixel mixture model will solve. But is the solution realistic? Solutions can occur with negative feature areas or impossibly low or high temperatures. We can take these and use them. However, it is up to the analyst to decide, through comparison with, and knowledge gained from, ground truth data (i.e., field measurements of the thermal structures at the feature type under consideration) to assess whether the solution is plausible or not, as can be done using the thermal structure blueprints provided in Electronic Supplement 1. For example, solution suggesting surface temperatures of 1500 °C at a basaltic system, where absolute maximum temperatures of 1200 °C are expected, suggests that the result is an artifact of the model. Likewise, a solution that yields a crust temperature of 25 °C for a proximal portion of an active basaltic lava channel at the height of eruption again suggests that the model has solved, but the results are inappropriate. In such cases we need to question and revise the model applied and assumptions used, and try again; accepting that, in some cases – given the complexity of volcanic thermal surfaces and the limits of the data – a realistic solution may not be possible.

References

- Flynn, L. P., Mougini-Mark, P. J. and Horton, K. A. (1994). Distribution of thermal areas on an active lava flow field: Landsat observations of Kilauea, Hawaii, July 1991. *Bulletin of Volcanology*, **56**, 284–296.
- Harris, A. J. L., Wright, R. and Flynn, L. P. (1999). Remote monitoring of Mount Erebus Volcano, Antarctica, using Polar Orbiters: Progress and Prospects. *Internal Journal of Remote Sensing*, **20**(15&16), 3051–3071.